

Figure 2 CTGF mRNA injections induce anti-BMP phenotypes in *Xenopus* embryos. **a–d**, Dorsal views of tail-bud stage embryos. **a**, Uninjected; **b**, CTGF mRNA (150 pg); **c**, CTGF-CR mRNA (800 pg) and **d**, CTGF-ΔCR mRNA (500 pg) injected ventrally at 4-cell stage. **e**, RT-PCR analysis of whole embryo (WE), animal cap uninjected (AC control) or injected with 50 pg of CTGF mRNA per blastomere at the 4-cell stage (AC CTGF). Animal cap explants were dissected at stage 9 and cultured until sibling embryos reached stage 26. *EF1-α* was used as RNA loading control and *αActin* to monitor mesoderm in the ectodermal explants. Three-day tadpoles, **f**, uninjected, **g**, injected with 50 pg of CTGF mRNA into the animal region of each blastomere at 4-cell stage. Cement-gland marker *XAG-1*, **h**, uninjected, **i**, injected with 150 pg of CTGF mRNA per blastomere at 4-cell stage. **j–o**, *in situ* hybridization at neural plate stage for *Sox-2* (**j–l**) and *Msx-1* (**m–o**); **j**, **m**, Uninjected embryos; **k**, **n**, injected with 50 pg of CTGF; **l**, **o**, 150 pg of CTGF-CR mRNA injected per blastomere at 4-cell stage.

(Fig. 2e). In addition, CTGF caused a weaker induction of the pan-neural marker *N-CAM* and downregulation of the epidermal markers *Msx-1* and *Cytokeratin* (Fig. 2e). Microinjection of CTGF mRNA into the animal pole resulted in embryos with enlarged heads, shortened trunk and tail structures (Fig. 2f, g), and expanded expression of the anterior cement-gland marker *XAG-1* (Fig. 2h, i). In CTGF-injected embryos analysed at the neurula stage, the expression domain of the neural-plate marker *Sox-2* was expanded (Fig. 2j, k) and, reciprocally, the expression domain of *Msx-1*, which demarcates the border between the neural plate and epidermis, was displaced laterally (Fig. 2m, n). Embryos injected with CTGF-CR also developed with expanded neural plates (Fig. 2l, o). We conclude from these *in vivo* results that CTGF can induce anti-BMP phenotypes in microinjected *Xenopus* embryos through its CR domain.

To test whether CTGF and BMP interacted biochemically, Flag-epitope-tagged constructs of full-length CTGF, CTGF-CR, CTGF-ΔCR and the C terminus of CTGF (CTGF-CT) were generated and the proteins produced in cultured cells (Fig. S2). To produce CTGF in sufficient amounts for biochemical experiments we generated a *Drosophila melanogaster* S2 stable cell line secreting Flag-tagged

Xenopus CTGF. Under these conditions the protein was full length and could be affinity-purified via its Flag tag (Fig. S2). Immunoprecipitation assays showed that full-length CTGF, like the positive control chordin, could bind BMP4 in solution (Fig. 3a, lanes 2, 3). Using a monoclonal antibody that is entirely specific for BMP4 (ref. 11), we showed in western blots that the binding of BMP4 to CTGF could be competed by an excess of BMP2 or TGF-β1 but not by IGF-1 (Fig. 3b, lanes 2–5). The interaction between CTGF and BMP4 was direct, because in chemical crosslinking experiments, full-length CTGF or the CR domain of CTGF (CTGF-CR) could be crosslinked to BMP4, forming complexes of the expected molecular weights (Fig. 3c, lanes 2, 5). Conversely, CTGF constructs lacking the CR domain (CTGF-ΔCR and CTGF-CT) were unable to form complexes with BMP4 (Fig. 3c, lanes 3, 4). The observation that binding of BMP4 to CTGF could be partially competed by TGF-β1 (Fig. 3b, lane 4) suggested that CTGF might also bind TGF-β1. Chemical crosslinking experiments showed that TGF-β1 could also bind directly to CTGF or to CTGF-CR (Fig. 3d, e). The binding affinity of CTGF for BMP4 and TGF-β1 was determined by surface plasmon resonance (SPR) analysis, a method used previously to evaluate real-time interactions between BMP and follistatin¹². Kinetic measurements using different concentrations of CTGF yielded dissociation constants (K_D) of 5 nM for BMP4 and of 30 nM for TGF-β1 (Fig. 3f). We conclude from these biochemical studies that CTGF can directly bind BMP4 and TGF-β1 through its CR domain, and has a higher affinity for BMP4 than for TGF-β1.

Purified CTGF inhibited BMP signalling in 10T1/2 cells^{13,14} (Fig. 4a, b). Increasing amounts of CTGF inhibited the alkaline phosphatase (AP) activity induced by 2.5 nM BMP4 in a dose-dependent manner (Fig. 4b) with 50% inhibition (IC_{50}) at approximately 12 nM. The phosphorylation of Smad1 induced by 0.5 nM BMP4 was inhibited by the addition of 20 nM CTGF (Fig. 4c, lanes 2 and 3) to human 293T cell cultures¹⁵. Interestingly, an excess of BMP4 (10 nM) was able to quench the antagonistic effect of CTGF on BMP4 action (Fig. 4c, lanes 4 and 5). To address the molecular mechanism by which CTGF inhibited BMP4 signalling we next examined the effect of CTGF on the binding of BMP4 to its cognate receptor¹⁶. Increasing amounts of CTGF antagonized BMP4 binding to a recombinant type Ia BMP-receptor-Fc fusion protein, as shown by western blot analysis with anti-BMP4 antibody (Fig. 4d, lanes 2–5). We conclude that binding of BMP4 to CTGF inhibits BMP signalling by preventing the binding of BMP4 to its cognate receptor. This molecular mechanism of action is analogous to that of the BMP antagonist chordin¹³.

CTGF did not inhibit binding of TGF-β1 to a TGFβ-receptor II-Fc (TβRII-Fc) recombinant protein. On the contrary, preincubation with CTGF increased the crosslinking of [¹²⁵I]TGF-β1 to recombinant TβRII-Fc in solution (Fig. 5a). CTGF also enhanced the binding of [¹²⁵I]TGF-β1 to endogenous receptors on the surface of cultured cells. Using the method of Massague¹⁷, it was found that crosslinking of TGF-β to all three TGF-β interacting proteins — betaglycan, TβRII and TβRI — increased in the presence of CTGF (Fig. 5b). Because CTGF binds TGF-β1 with relatively low affinity (with a K_D value of only 30 nM, Fig. 3f), it is conceivable that CTGF may function as a chaperone to modify the conformation or solubility of TGF-β1 and facilitate presentation to its cognate receptors, which have affinities in the picomolar range¹⁷. Signalling by TGF-β1 was also increased by CTGF. At low TGF-β1 concentrations, CTGF potentiated the phosphorylation of Smad2 induced by TGF-β1 (Fig. 5c, lanes 2 and 3) in fetal mink lung (Mv1Lu) cell cultures. At higher concentrations of TGF-β1, CTGF did not increase Smad2 phosphorylation, indicating that CTGF serves to potentiate the effects of limiting amounts of TGF-β1 and has no detectable effects of its own on these cells (Fig. 5c, lanes 4–6). In addition, a TGF-β reporter gene¹⁸ was induced 6–10-fold by as little as 3 nM CTGF (Fig. 5d). TGF-β1 was required, as CTGF alone did not induce reporter-gene expression, even at 45 nM (Fig. 5d).

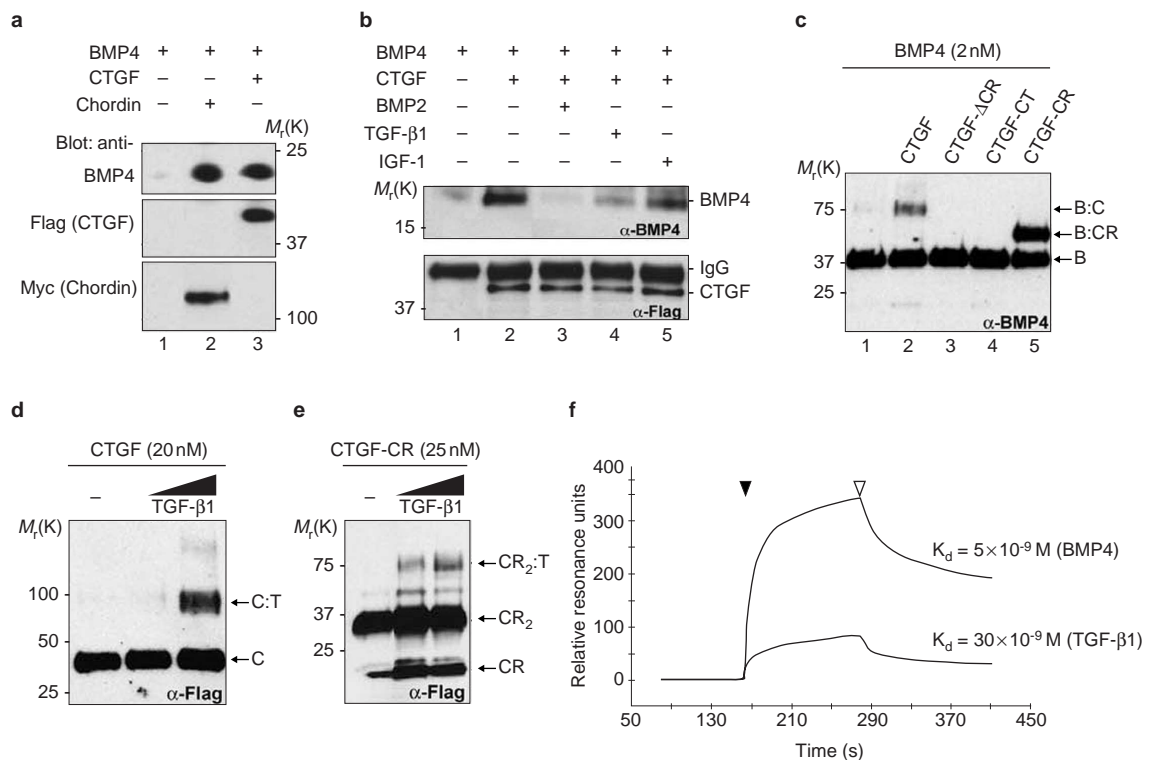


Figure 3 CTGF binds BMP4 and TGF-β1 through the CR domain. **a**, Western-blot analysis of BMP4 (5 nM) bound to CTGF (10 nM, lane 3) or chordin (5 nM, lane 2) after immunoprecipitation (IP) as described previously⁴. To determine IP effectiveness, the same blots were subsequently probed with anti-Flag antibody for CTGF and anti-myc antibody for chordin. **b**, Competition of BMP4 (5 nM) bound to CTGF (10 nM) by IP in the absence (lane 2) or presence of 20-fold molar excess of BMP2 (lane 3), TGF-β1 (lane 4) or IGF-1 (lane 5). CTGF IP efficiency was monitored with anti-Flag antibody. **c**, Chemical crosslinking of CTGF and CTGF mutant constructs to BMP4. Membrane was probed with anti-BMP4 antibody. Bands corresponding to BMP4 dimer (B), BMP4-CTGF complex (B-C) and BMP4:CTGF-CR complex (B-CR)

are indicated. **d**, **e**, Western blot probed with anti-Flag antibody after chemical crosslinking of CTGF and CTGF-CR to TGF-β1. Bands corresponding to CTGF monomer (C), CTGF-TGF-β1 (C-T) complex, and to CTGF-CR monomer (CR), to the dimer of CTGF-CR (CR₂) and to the complex of a dimer of CTGF-CR with TGF-β1 (CR₂-T) are indicated. The TGF-β1 was added at 25 nM and 50 nM. **f**, Sensorgrams of SPR analyses showing the binding of purified CTGF to BMP4 or to TGF-β1. CTGF protein was run (black arrowhead) over BMP4 or TGF-β1 sensor chips. After CTGF flow ended (white arrowhead), dissociation was monitored by a decrease in the resonance units. Kinetic experiments were performed using CTGF concentrations ranging between 6.5 nM and 210 nM of full-length CTGF.

The synergy between CTGF and TGF-β1 was accompanied by a striking and unexpected morphological change in the cultures. Spherical aggregates of cells were observed in Mv1Lu cells treated with TGF-β1 and purified CTGF, but not when treated with either factor on its own (Fig. 5e and Fig. S3 in the Supplementary Information). These effects of CTGF were not caused by a blockade of endogenous BMP signals, because addition of 10 nM chordin or BMPRIa-Fc (which are sufficient to inhibit BMP4 signalling in cell culture, data not shown) together with TGF-β1 did not induce spherical structures in Mv1Lu cells (Fig. 5e). In embryonal carcinoma P19 cells similar structures were induced by CTGF alone (Fig. 5f), presumably because these cells produce endogenous TGF-β (see the legend to Fig. S3). The cell aggregates were positive for platelet-endothelial cell-adhesion molecule (PECAM-1) and for vWF (Fig. 5f and Fig. S3). Although these molecules are markers for endothelial cells, it has recently been reported that PECAM-1 is not entirely specific for blood vessels¹⁹ and therefore the determination of whether the spherical structures reported here correspond to blood-vessel-like structures must await further experimentation. We conclude that CTGF protein enhances TGF-β1 signalling by several criteria, including receptor and cell-surface binding, Smad2 phosphorylation, activation of gene expression, and differentiation of cultured cell lines.

Although multiple physiological roles have been proposed for CTGF, its signalling pathway remains unknown. CTGF can bind

to low-density lipoprotein receptor-related protein and integrins^{20,21}, but the consequences of these interactions on downstream signaltransduction pathways are not known. The results reported here indicate that CTGF signals in part through the binding of BMP4/2 and TGF-β1 in the extracellular space. We find that CTGF inhibits BMP but activates TGF-β1 signalling. TGF-β is a well-known inducer of extracellular matrix (ECM) components such as collagen and fibronectin^{22,23}. The CTGF gene may participate in this event, as its promoter contains a TGF-β response element^{24,25}. In support of this view, collagen deposition and anchorage-independent growth induced by TGF-β in fibroblasts can be inhibited by adding neutralizing antibodies against CTGF^{23,26}, indicating a synergistic relationship between CTGF and TGF-β. The function of the other domains in CTGF remains to be investigated: the IGF domain has been shown to bind IGF although this interaction is of low affinity (ref. 27 and our unpublished observations), TSP-1 domains have been implicated in extracellular matrix and vascular endothelial growth factor (VEGF) binding^{28,29}, and the cystine-knot module may contribute a dimerization motif or additional signalling capabilities³⁰. In conclusion, the results presented here suggest a molecular mechanism for CTGF function by which this protein can activate TGF-β signalling and inhibit BMP activity by directly binding to these growth factors in the extracellular space through its Chordin-like domain. □

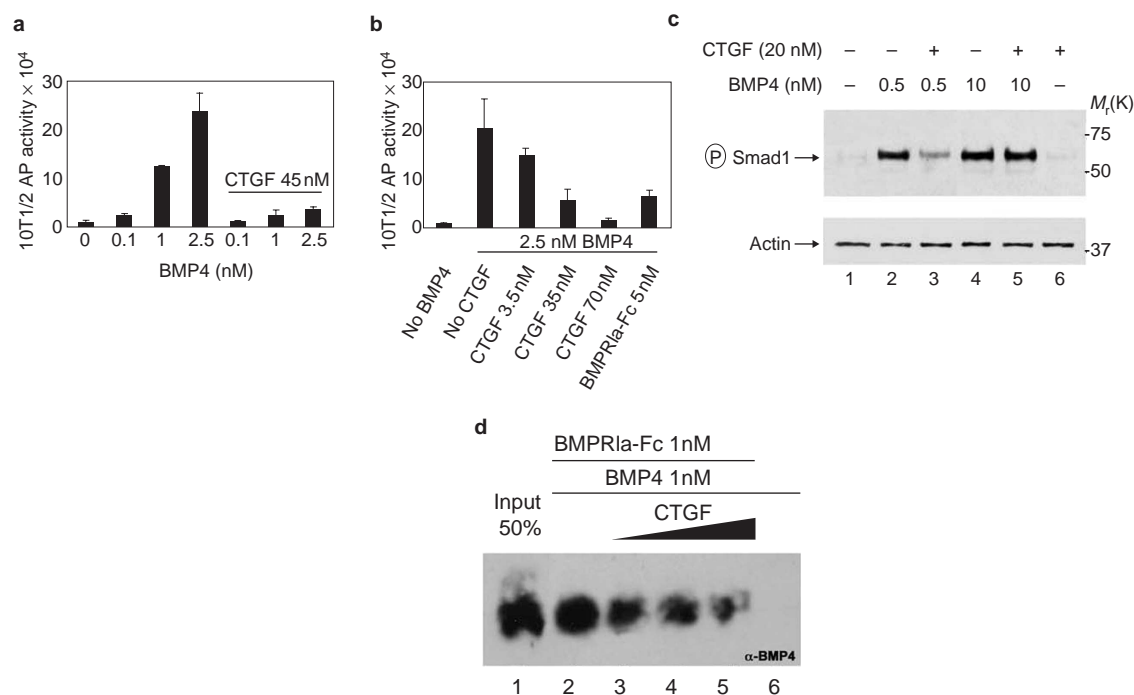


Figure 4 CTGF antagonizes BMP4 signalling by inhibiting receptor binding. **a**, Dose-dependent induction of alkaline phosphatase (AP) by BMP4 in 10T1/2 cells is inhibited by CTGF. **b**, Adding increasing amounts of CTGF inhibits AP induced by 2.5 nM of BMP4. We estimate that CTGF can block BMP4 activity with an IC₅₀ of about 12 nM. Error bars represent standard deviations of triplicate samples. Experiments were independently performed three times. **c**, Inhibition of Smad1 phosphorylation in 293T cells by CTGF at low, but not high, BMP4 concentrations.

d, CTGF inhibits binding of BMP4 to its cognate receptor. BMP4 (1 nM) was pre-incubated 1 h at room temperature with 10, 25 and 50 nM (black triangle) of affinity-purified CTGF (lanes 3–5), and BMPRIa-Fc was added at 1 nM for 2 h. Lane 1 corresponds to the loading of 50% of the total BMP4 used in each reaction. Lane 6 shows negative control of BMP4 binding to protein A beads in the absence of the BMPRIa-Fc.

Methods

DNA constructs and embryo manipulations

The complete open reading frame of *Xenopus CTGF* was amplified by PCR from cDNA of stage 25 embryos using the following primers: forward 5'-AAA CTC GAG GAA CTA ATC TGC TGC TGT-3' and reverse 5'-AAA TCT AGA TGT GTT TCT CTG CCT CTA-3', based on the sequence from GenBank accession number U43523 entered by M. L. King and Z. Ying in 1997. The PCR product was cloned in the expression vector *pCS2+*. Epitope-tag subclones were generated by amplifying *CTGF* lacking the signal peptide and inserting the fragment in-frame into *pCS2+* containing a chordin signal peptide until Ala41, followed by the Flag-tag sequence (*pchd-Flag*). The primers used for Flag-tagged full-length CTGF or deletion mutants were as follows: CTGF 5'-AAA CTC GAG GAG TGT AAT GGG GAA T-3' and 5'-AAA TCT AGA TGT GTT TCT CTG CCT CTA-3'; CTGF-CR 5'-AAA CTC GAG GCC CCT TGT TGT GTT CCG-3' and 5'-AAA TCT AGA TAG CGC GGA TTA GGG ATG GA-3'; CTGF-CT, 5'-AAA CTC GAG GGT CCT GAT CCA TCC CTA-3' and T7 primer. CTGF-ΔCR was generated by deletion of sequences between Ala95 and Ala191 of CTGF by PCR mutagenesis. Detailed protocols for embryo fertilizations, *in situ* hybridization and RT-PCR can be found at <http://www.hhmi.ucla.edu/derobertis/index.html>.

Protein purification, immunoprecipitation and crosslinking

Flag-tagged secreted proteins were obtained by transient transfection of human 293T cells or from *Drosophila* S2 cells stably expressing CTGF (Fig. S2). Full-length Flag-CTGF from S2 cells was affinity-purified with anti-Flag M2 affinity gel column and eluted with Flag peptide according to manufacturer's directions (Sigma, St Louis, MO). Culture medium obtained from *Drosophila* S2 cells transfected with empty vector was purified in the same way and used as negative control in all experiments. Protein concentrations were determined using bovine serum albumen (BSA) standards stained with Coomassie blue in SDS-polyacrylamide gel electrophoresis (SDS-PAGE). Immunoprecipitation analyses and chemical crosslinking with disuccinimidyl suberate (DSS) were performed as described previously^{4,13}.

TGF-β-receptor binding

[¹²⁵I]-TGF-β1 (specific activity 3000 Ci/mmol, NEN) was crosslinked to recombinant TGF-β-receptor II-Fc (TβRII-Fc) (R&D systems, Minneapolis, MN). Different concentrations of [¹²⁵I]-TGF-β1 were pre-incubated for 1 h in absence or presence of 10 nM of purified CTGF. 1 nM of TβRII-Fc was added to the reactions for 30 min and the samples were crosslinked with DSS for 30 min⁴. Binding of [¹²⁵I]-TGF-β1 to cell surface receptors of NRK9F cultured cells was performed as described previously¹⁷. Briefly, 100 pM [¹²⁵I]-TGF-β1 was pre-incubated with or without 6 nM of purified CTGF for 1 h. Proteins were added to semi-confluent normal rat kidney (NRK) cells pre-equilibrated in binding

buffer (128 mM NaCl, 5 mM KCl, 5 mM MgSO₄, 1.2 mM CaCl₂, 50 mM HEPES, 2 mg ml⁻¹ BSA, pH 7.5) and incubated for 4 h at 4 °C on an oscillating platform at 120 rpm. After extensive washes with ice-cold binding buffer, DSS was added in binding buffer without BSA for 15 min at 4 °C. Cells were extracted in detachment buffer (0.25 M sucrose, 10 mM Tris, 1 mM EDTA, pH 7.4, 0.3 mM PMSF), sedimented by centrifugation and the pellets solubilized with solubilization buffer (125 mM NaCl, 10 mM Tris, 1 mM EDTA, pH 7.0, 1% Triton X-100). Cell debris were removed by centrifugation, and samples were subjected to SDS-PAGE.

Surface plasmon resonance (SPR) analysis

Real-time binding experiments were performed on the Biacore 2000 apparatus (Biacore AB, Uppsala, Sweden) as described previously¹³. Carrier-free recombinant human BMP4 and TGF-β1 from human platelets (R&D Systems) were immobilized on the sensor-chip surface (CM5, certified grade, Biacore AB). HBS-EP buffer (10 mM HEPES pH 7.4, 150 mM NaCl, 3 mM EDTA and 0.005% v/v surfactant P20) was used as running buffer.

Cell culture assays and immunocytochemistry

Alkaline phosphatase (AP) induction assay¹³ was performed in the multipotent mesodermal cell line 10T1/2 (ATCC) using the fluorescent substrate 4-methyl umbelliferyl-phosphate (Sigma). AP values were normalized using the amount of protein in each tissue-culture well (Bio-Rad Dc protein kit). Mink lung epithelial cells (Mv1Lu – CCL 64, ATCC) were cultured in alpha-minimal essential media (MEM; Gibco, Grand Island, NY) supplemented with 10% foetal bovine serum. Cells plated in 96-well plates were transiently co-transfected with 0.1 μg of *p3TP-lux* (ref. 18) and 0.015 μg of *pBSKSβ-gal* expression plasmid using FuGENE (Roche, Indianapolis, IN) as a transfection reagent. Before growth factors were added, cells were washed with phosphate buffer saline and pre-incubated for 2 h with alpha-MEM containing 2% NuSerum (BD Biosciences, San Jose, CA). Growth factors diluted in alpha-MEM containing 2% NuSerum were pre-incubated at room temperature for 1 h before they were added to cells. After 18 h cells were lysed in Reporter Lysis Buffer (Promega, Madison, WI), and enzyme activity measured using the Luciferase Assay System and the β-Galactosidase Enzyme Assay System (Promega). Enzyme activities were measured in a microplate luminometer and enzyme-linked immunosorbent assay (ELISA) plate reader, respectively. Smad phosphorylation was detected on western blots using 1:6000 dilution of anti-phosphoSmad1 (specific for Smad 1, 5 and 8, gift of C. H. Heldin), 1:500 dilution of anti-phosphoSmad2 (Upstate Biotechnology, Waltham, MA), and 1:400 actin antibodies (Sigma) for protein loading controls. Purified growth factors were premixed for 1 h in serum-free medium (DMEM, F12, Iscove's, 1:1:1) at room temperature, and added to 80% confluent 293T or Mv1Lu cells for 2 h. Immunocytochemistry was performed with an endothelial-specific anti-CD31 (PECAM-1) monoclonal antibody²² (MEC 13.3, Pharmingen, San Diego, CA) diluted 1:400, and an anti-β-actin polyclonal antibody (Dako Co., Burlingame, CA) diluted 1:200. Staining was visualized after incubation with secondary

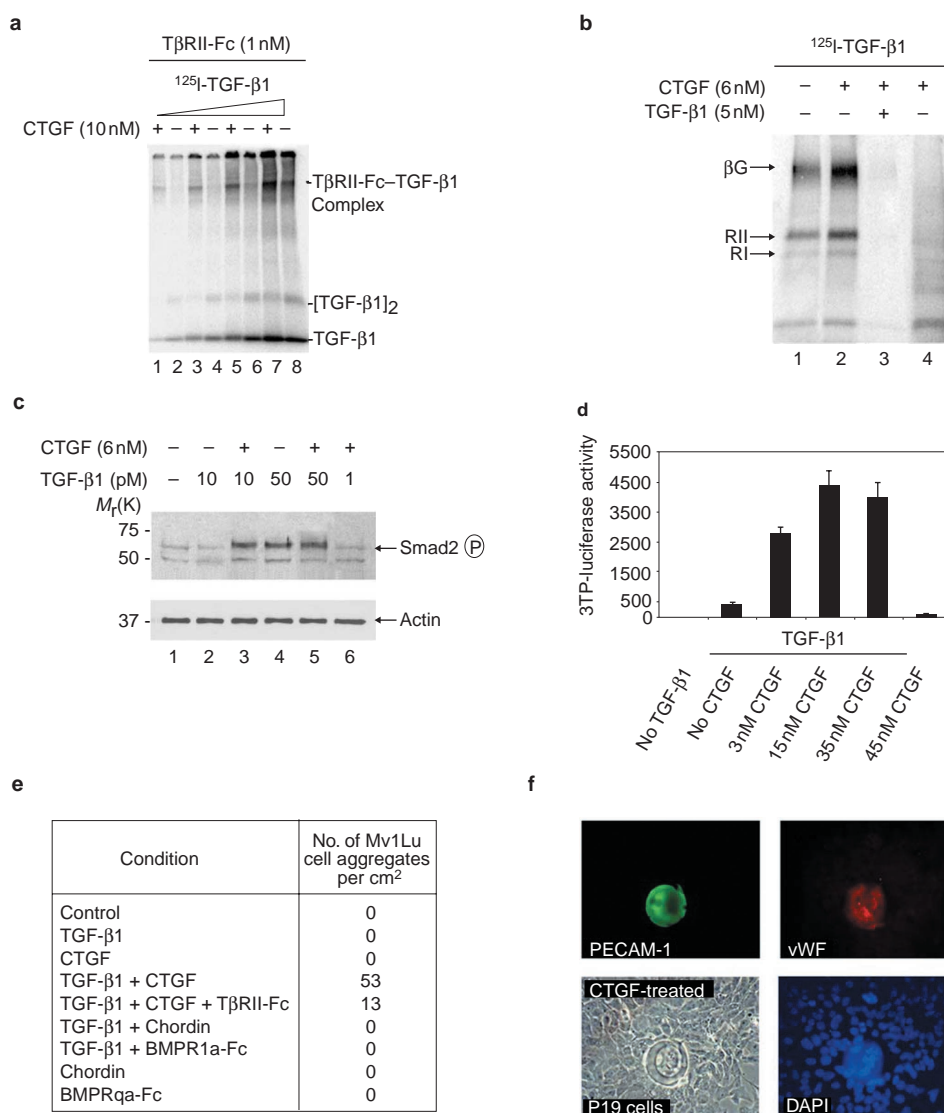


Figure 5 CTGF potentiates TGF-β1 receptor binding and signalling.

a, Crosslinking of [¹²⁵I]-TGF-β1 to 1 nM TGF-β receptor Fc fusion protein (TβRII-Fc) in the presence (+) or absence (-) of 10 nM purified CTGF. The TβRII-Fc-TGF-β1 complex is seen in the upper part of the gel. Different concentrations of [¹²⁵I]-TGF-β1, ranging from 10 pM to 0.5 nM, were used. **b**, Labelling of cell-surface proteins by [¹²⁵I]-TGF-β1 in NRK cells after chemical crosslinking with DSS. [¹²⁵I]-TGF-β1 (100 pM) was pre-incubated 1 h with (+) or without (-) 6 nM CTGF before adding for receptor binding¹⁷. Specific binding was shown by competition with 50-fold unlabelled TGF-β1 (lane 3). Lane 4 shows negative control crosslinking of CTGF, and [¹²⁵I]-TGF-β1 in the absence of cells. The three major cell surface TGF-β receptors¹⁷ are indicated: betaglycan (βG, 250 kDa), TGF-β-receptor II (TβRII, 80 kDa) and TGF-β-receptor I (TβRI, 68 kDa). **c**, Two hours after addition of proteins, Smad2 phosphorylation in Mv1Lu cells was stimulated by 6 nM CTGF in the presence of 10 pM TGF-β1. This effect was not seen when TGF-β1 was increased fivefold. Lane 6 shows that CTGF

has no effect on its own. Note that Smad2 phosphorylation was induced at lower concentrations of TGF-β1 than those required in reporter-gene or cell-differentiation assays (see below), perhaps reflecting the shorter treatment times involved. **d**, Luciferase activity 36 h after transfection of Mv1Lu cells with the TGF-β inducible reporter *p3TP-lux*. Constant TGF-β1 and different concentrations of CTGF were used. Note that CTGF protein stimulates TGF-β1 signalling even when as little as 3 nM is used. **e**, Number of spherical cell aggregates per square centimeter observed in Mv1Lu cells after 12 h of treatment with different growth factors as described above. The concentrations of CTGF and TGF-β1 were 3 nM and 200 pM, respectively. Note that the BMP inhibitors Chordin and BMPRIa-Fc could not replace CTGF, and that soluble TGFRII-Fc inhibited spherical aggregate formation. **f**, Immunofluorescence showing the formation of spherical cell aggregates in P19 embryonal carcinoma cells treated with 5 nM CTGF. P19 cell aggregates were positive for PECAM-1 and vWF.

antibodies conjugated to fluorescein isothiocyanate (FITC) or Cy3 (Jackson ImmunoResearch Laboratories) using fluorescent microscopy. Coverslips were mounted in Vectashield mounting media containing DAPI (Vector, Carpinteria, CA). Negative controls were performed by omitting the primary antibody during the immunostaining reaction.

ACKNOWLEDGEMENTS

We thank K. M. Lyons and S. Ivkovic for unpublished information, K. Masuhara and C.H. Heldin for antibodies, J. Massague for reporter plasmid, Naoto Ueno for the protocol to immobilize BMP4 to Biacore chips, M. L. King and Z. Ying for entering the CTGF full-length sequence in GenBank, S.-Y. Li

and A. Cuellar for technical assistance, and C. Coffinier, E. Delot, J. I. Kim, J. Larrain, K. M. Lyons, M. Oelgeschläger, E. Pera, O. Wessely for discussions and comments on the manuscript. J.G.A. was a Latin American PEW fellow. This work was supported by the National Institutes of Health (R37 HD21502-16). E.M.D.R. is an Investigator of the Howard Hughes Medical Institute. Correspondence and requests for material should be addressed to E.M.D.R. Supplementary information is available on *Nature Cell Biology's* website (<http://cellbio.nature.com>).

COMPETING FINANCIAL INTERESTS

The authors declare that they have no competing financial interests.

RECEIVED 28 MARCH 2002; REVISED 10 MAY 2002; ACCEPTED 24 MAY 2002;
PUBLISHED 22 JULY 2002

1. Moussad, E. E. & Brigstock, D. R. *Mol. Genet. Metab.* **71**, 276–292 (2000).
2. Abreu, J., Coffinier, C., Larrain, J., Oelgeschlager, M. & De Robertis, E. M. *Gene* **287**, 39–47 (2002).
3. Zhu, Y., Oganessian, A., Keene, D.R. & Sandell, L. J. *J. Cell Biol.* **144**, 1069–1080 (1999).
4. Larrain, J. *et al. Development* **127**, 821–830 (2000).
5. Nakayama, N. *et al. Dev. Biol.* **232**, 372–387 (2001).
6. Sakuta, H. *et al. Science* **293**, 111–115 (2001).
7. Hunt, L.T. & Barker, W.C. *Biochem. Biophys. Res. Commun.* **144**, 876–882 (1987).
8. Bork, P. *FEBS Lett.* **327**, 125–130 (1993).
9. Smith, W.C. & Harland, R.M. *Cell* **70**, 829–840 (1992).
10. Sasai, Y. *et al. Cell* **79**, 779–790 (1994).
11. Masuhara, K. *et al. Bone* **16**, 91–96. (1995).
12. Iemura, S. *et al. Proc. Natl. Acad. Sci. USA* **95**, 9337–9342 (1998).
13. Piccolo, S., Sasai, Y., Lu, B. & De Robertis, E. M. *Cell* **86**, 589–598 (1996).
14. Katagiri, T. *et al. Biochem. Biophys. Res. Commun.* **172**, 295–299 (1990).
15. Persson, V. *et al. FEBS Lett.* **434**, 83–87 (1998).
16. Larrain, J. *et al. Development* **128**, 4439–4437 (2001).
17. Massagué, J. *Methods Enzymol.* **46**, 174–195 (1987).
18. Wrana, J. L. *et al. Cell* **71**, 1003–1014 (1992).
19. Robson, P., Stein, P., Zhou, B., Schultz, R. M. & Baldoïn, H. S. *Dev. Biol.* **234**, 317–329 (2001).
20. Segarini, P. R. *et al. J. Biol. Chem.* **276**, 40659–40667 (2001).
21. Kireeva, M. L. *et al. Exp. Cell Res.* **233**, 63–77 (1997).
22. Roberts, A. B. *et al. Proc. Natl. Acad. Sci. USA* **83**, 4167–4171 (1986).
23. Frazier, K., Williams, S., Kothapalli, D., Klapper, H. & Grotendorst, G. R. *J. Invest. Dermatol.* **107**, 404–411 (1996).
24. Grotendorst, G. R., Okochi, H. & Hayashi, N. *Cell Growth Differ.* **7**, 469–480 (1996).
25. Holmes, A. *et al. J. Biol. Chem.* **276**, 10594–10601 (2001).
26. Kothapalli, D., Frazier, K. S., Welply, A., Segarini, P. R. & Grotendorst, G. R. *Cell Growth Differ.* **8**, 61–68 (1997).
27. Kim, H. S. *et al. Proc. Natl. Acad. Sci. USA* **94**, 12981–12986 (1997).
28. Adams, J. C. & Tucker, R. P. *Dev. Dyn.* **218**, 280–299 (2000).
29. Inoki, I. *et al. FASEB J.* **16**, 219–221 (2002).
30. Pearce, J. J., Penny, G. & Rossant, J. *Dev. Biol.* **209**, 98–110 (1999).

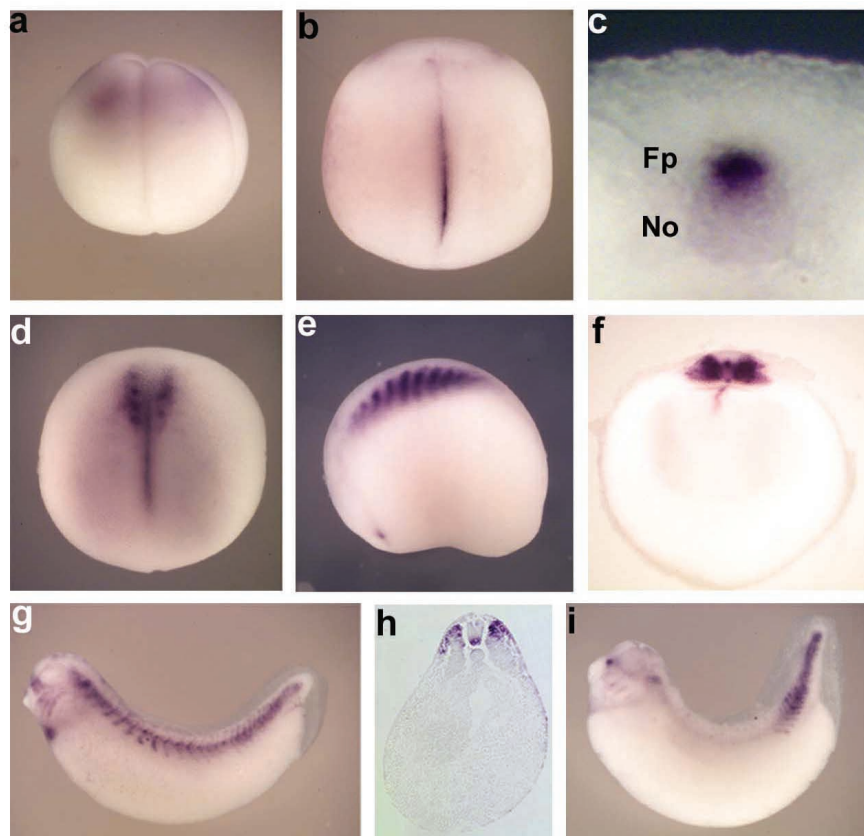


Figure S1 **Expression pattern of CTGF in *Xenopus* embryogenesis detected by *in situ* hybridization.** **a**, lateral view of four-cell stage embryo; **b**, dorsal view of early neural plate stage; **c**, close up of section at neural plate stage, note staining in floor plate (Fp) and notochord (No); **d**, **e**, dorsal and lateral view at the late neurula stage showing expression in somites; **f**, cross-section of a late neurula; **g**, **i**, lateral view of tailbud stage embryos; **h**, section through early tailbud stage. The sequence of *Xenopus* CTGF had been presented in the Genbank database (accession # U43523), but its expression during development had been not described. Our *in situ* hybridization analysis revealed the presence of maternal CTGF transcripts in the animal region of four-cell stage embryos and very little expression during gastrulation (panel **a** and data not shown). At early neurula stage zygotic transcripts were detected in the dorsal midline, mainly in the floor plate, and at lower levels in the underlying notochord (**b-c**). CTGF was also expressed throughout the developing somites at the late neurula stage and later became restricted to the

dorsal aspect of the somite (**f-i**). At tailbud stage additional expression domains were seen in the developing heart, nasal placode and branchial arches (**g**, **i**). Thus, CTGF is expressed at various sites during early *Xenopus* development, including dorsal tissues known to be involved in embryonic patterning.

An antisense morpholino oligonucleotides directed against the immediate 5' leader region of CTGF mRNA (sequence: GTACAGCAGCAGATTAGTTCTCTTC) was microinjected into 2-cell *Xenopus* embryos. No specific morphological phenotypes were observed at 8, 10 or 80 ng of oligonucleotides per embryo (n=34, 33 and 19, respectively). The CTGF gene has been inactivated in the mouse by S. Ivkovic and K. M. Lyons (UCLA) and although the mice die perinatally, the overall body patterning is not affected by the mutation (personal communication). Thus, even if the morpholino caused phenotypes similar to those seen in mouse, we would not have expected to observe them by examination of *Xenopus* embryos at the tailbud tadpole stage.

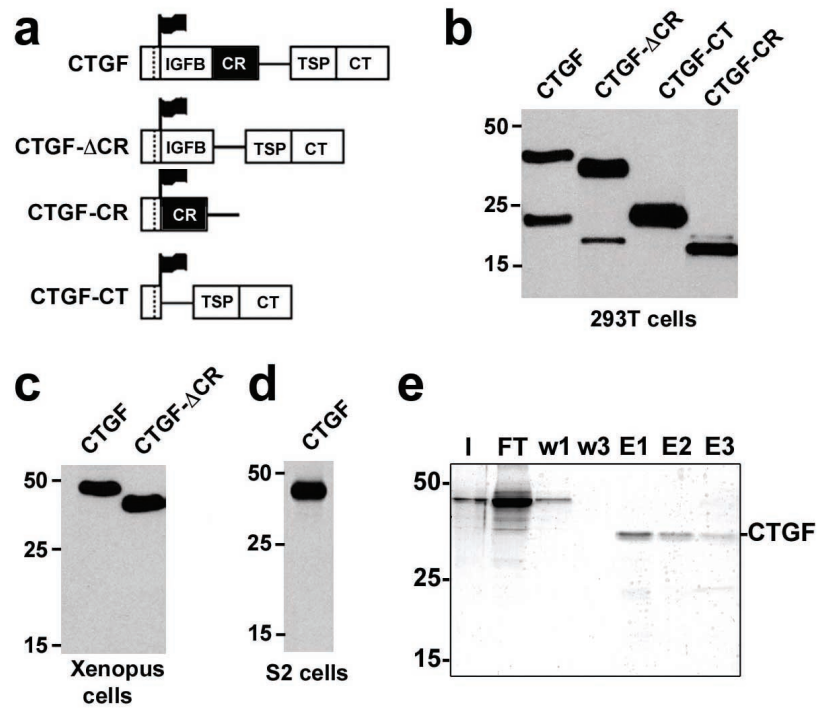


Figure S2 CTGF constructs and expression of CTGF proteins in human 293T cells, *Xenopus* embryos and *Drosophila* S2 cells. **a**, Schematic representation of full-length Flag epitope-tagged CTGF containing its four structural modules: the IGF binding domain (IGFB), the CR/vwc domain, the Thrombospondin-1 domain and the C-terminal cystine knot (CT). Mutants lacking the CR domain (CTGF- Δ CR and CTGF-CT), or consisting of the CR domain only (CTGF-CR) are shown. After cleavage of the signal peptide (dashed line), proteins retain twenty amino acids of the N-terminal part of Chordin (N-chd) followed by a Flag epitope sequence. The Chordin epitope tag allowed us to perform immunoprecipitation assays using an anti-N-chd polyclonal antibody¹. **b**, Western blot using anti-Flag antibody of the proteins represented in the previous panel. Proteins were produced by transient transfection in 293T cells. Note that full-length CTGF and CTGF- Δ CR are partially cleaved and N-terminal fragments of 20 kDa and 18 kDa are generated, respectively. In other experiments the cleavage products were more prevalent than the unprocessed proteins. **c**, Expression of CTGF and CTGF- Δ CR in *Xenopus* embryonic cells. After injection of 100 μ g CTGF or CTGF- Δ CR mRNA into each blastomere of the four-cell stage *Xenopus*, animal halves were dissected at stage 9 and cells cultured overnight in calcium-magnesium-free media². Supernatant was collected, centrifuged and western blot using anti-Flag antibody performed. Note that the proteins produced in *Xenopus* were not cleaved. **d**, **e**, Large scale production and purification of full-length CTGF. Expression of Flag-CTGF in *Drosophila* S2 cells was performed as described³. Briefly, Flag-CTGF was sub-cloned into pUAST vector. To establish a cell

line 5 μ g of pUAST-CTGF were co-transfected with 1 μ g of pCoHygro (Invitrogen, for hygromycin resistance) and 5 μ g of pGal/pRmHa3, which contains the yeast Gal-4 protein under the control of the methalothioneine promoter. FuGENE (Roche) was used as transfection reagent and cells were selected with 250 μ g/ml of Hygromycin for 60 days. For protein secretion, 500 μ M of CuSO₄ was added to induce Gal4, which in turn induced CTGF expression via its UAS promoter. Note that the flag-CTGF produced by S2 cells is full-length. **e**, Flag-CTGF in S2 cell secreted media was purified by anti-Flag affinity gel (Sigma) column and eluted with Flag peptide (Sigma). Fractions were analyzed by SDS-PAGE stained with Coomassie blue. The gel was loaded with aliquots of the input in the column (I), of the flow through (FT), of the first and third washes (W1, W3) and of the three elutions (E1, E2 and E3). This method yielded approximately 100 μ g of pure CTGF per 30 ml of tissue culture medium. We found that the use of full-length affinity-purified CTGF was essential for the crosslinking, binding analysis and cell culture results shown here. The use of *Drosophila* S2 cells was crucial as human 293T cells secrete large amounts of proteolytically processed CTGF. It is not known whether this proteolytic cleavage, which occurs close to the center of the protein, has a biological role on CTGF function *in vivo*.

1. Larrain, J. *et al. Development* 127, 821–830 (2000).
2. Sive, H.L., Grainger, R.M. & Harland, R.M. *Early development of Xenopus laevis: A laboratory manual*, (Cold Spring Harbor Laboratory Press, New York, 2000).
3. Garrity, P.A. *et al. Neuron* 22, 707–717 (1999).

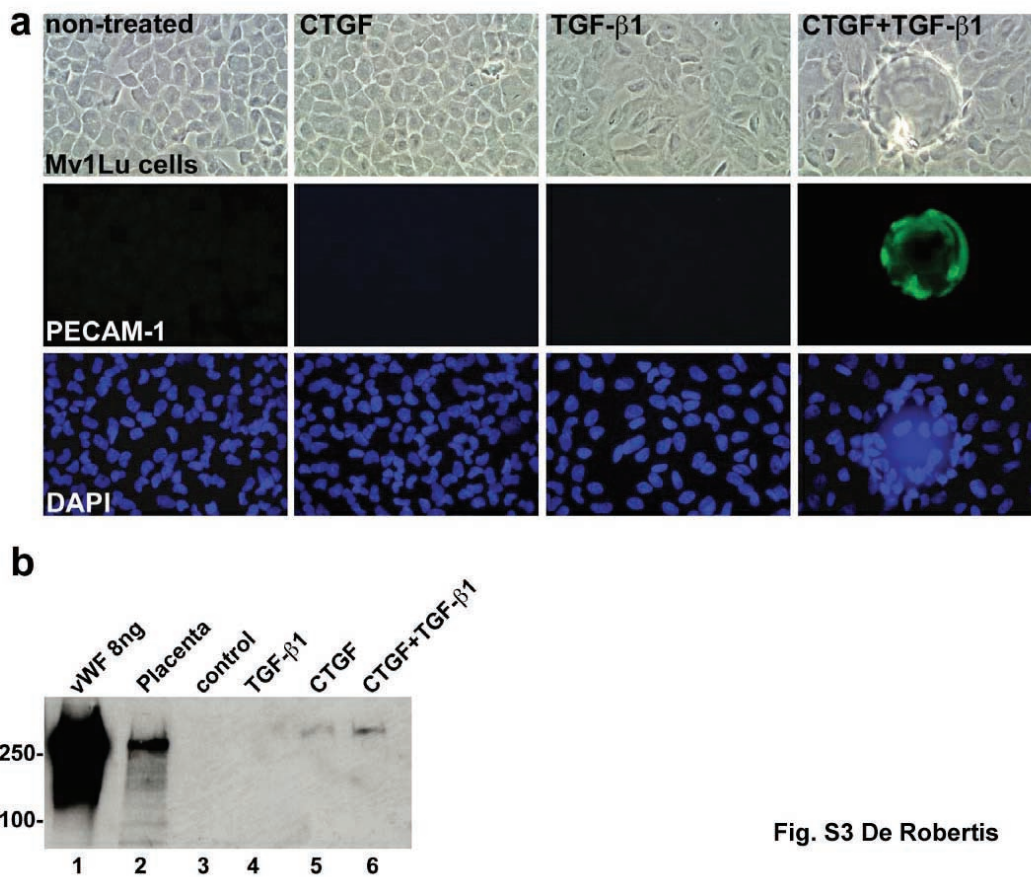


Fig. S3 De Robertis

Figure S3 **Synergy between TGF- β 1 and CTGF: Induction of striking morphological changes in Mv1Lu cells.** The combination of TGF- β 1 (0.2 nM) and CTGF (3 nM) induced spherical fluid-filled aggregates of Mv1Lu cells after 12 hours of culture (panel a). Previous studies have implicated TGF- β 1 and CTGF in angiogenesis¹⁻⁴. Immunocytochemistry was performed with the cell surface antigen⁵⁶ CD31, also known as platelet-endothelial cell adhesion molecule or PECAM-1. As shown in panel a, it was found that, indeed, the spherical aggregates were PECAM-1 positive. Spherical aggregates of PECAM-1-positive cells were not observed in Mv1Lu cells treated with TGF- β 1 or CTGF alone. Interestingly, in the pluripotent mouse embryonal carcinoma P19 cell line, addition of CTGF induced PECAM-1 positive cell aggregates without requiring the addition of TGF- β 1 (Fig. 5f). The mouse P19 cell structures were positive for PECAM-1 and for von Willebrand Factor, another endothelial marker (Fig. 5f). Panel b shows that increased amounts of vWF protein were detected in Mv1Lu cells treated with CTGF and TGF- β 1 by Western blot (lane 6); polyclonal anti-vWF (Dako Co) was used at 1:200, and purified vWF and mouse placental proteins were used as positive controls. Spherical structures are induced by CTGF alone in P19 cells (see Fig. 5f of main text) presumably because they express endogenous TGF- β 1 signals, since P19 cells have higher basal luciferase levels than Mv1Lu cells when transfected with a TGF- β -inducible reporter (data not shown). Mv1Lu cells have been very useful in TGF- β research because they have an intact TGF- β signal transduction pathway⁷ yet express low levels of endogenous TGF- β signals, which strongly inhibit their proliferation⁸. Further experiments will be required

to determine whether Mv1Lu cells, which were established from fetal mink lung tissue, are of endothelial origin. If the aggregates induced in Mv1Lu cells treated with CTGF and TGF- β 1 eventually are proven to form blood vessel-like spherical structures, they will provide a valuable system for the molecular dissection of the signals involved in angiogenesis. The CTGF gene has been inactivated by homologous recombination in the mouse and defects in angiogenesis are apparent in regions where CTGF and TGF- β are normally co-expressed, identifying CTGF as an essential mediator of angiogenesis *in vivo* (S. Ivkovic and K. M. Lyons personal communication). In gain-of-function experiments, CTGF ectopically expressed in chicken chorioallantoic membranes or in the rat cornea has been shown to promote angiogenesis and neovascularization^{3,4}. Even if it is eventually demonstrated that these remarkable structures are not of vascular nature, the formation of these cell aggregates may still provide an interesting *in vitro* system for the study of mesenchymal to epithelial transformation under the control of extracellular signals.

1. Roberts, A.B. *et al. Proc. Natl. Acad. Sci. U S A* 83, 4167-4171 (1986).
2. Dickson, M.C. *et al. Development* 121, 1845-1854. (1995).
3. Shimo, T. *et al. J. Biochem. (Tokyo)* 126, 137-145 (1999).
4. Babic, A.M., Chen, C.C. & Lau, L.F. *Mol. Cell. Biol.* 19, 2958-2966 (1999).
5. Baldwin, H.S. *et al. Development* 120, 2539-2553 (1994).
6. Vecchi, A. *et al. Eur. J. Cell Biol.* 63, 247-254 (1994).
7. Cheifetz, S., Like, B. & Massagué, J. *J. Biol. Chem.* 261, 9972-9978 (1986).
8. Tucker, R.F., Shipley, G.D., Moses, H.L. & Holley, R.W. *Science* 226, 705-707 (1984).